Activated Carbon for Electrochemical Supercapacitor and Water Filter

Abstract

Palm kernel shell and coconut shell have been combined in equal proportion to produce activated carbons for supercapacitor electrode and water filter. Microwave-assisted activation technique was employed for the production at a much shorter time (ranging from 5-10 min) and reduced cost compared to the conventional activation methods. Co-activator (mixture of NaCl and $CaCl_2$) was used to activate the sample for water filter with no added fillers while the sample for supercapacitor electrode was activated with KOH and NiO nanoparticles as fillers. Physical properties (such as density, ash content and moisture content) and Thermo-Gravimetric Analysis (TGA) were carried out to ascertain the quality of the activated carbons. In addition to the microstructural and structural investigations, surface functionalities, adsorption capability and electrochemical properties of the samples were also investigated. The surface chemistry, microstructure, structure and electrochemical properties of the produced activation carbon were investigated employing Fourier Transform Infra-Red (FTIR) Spectroscopy, Scanning Electron Microscopy (SEM), X-Ray Diffraction (XRD), Cyclic Voltammetry (CV) and Electrochemical Impedance Spectroscopy (EIS). The effectiveness of the activated carbon sample for water filter was tested for the removal of organic dye (methylene blue) from water contaminated with the organic dye via adsorption studies using the Freundlich model. Finally, the results; obtained from electrochemical studies, show that the activated carbon for supercapacitor electrode possesses good current response with high value of specific capacitance and it is a promising component for electrochemical devices.

Keywords: Agricultural wastes, Activated carbons, water filters, supercapacitor electrodes, energy storage and clean water.

Introduction

Palm kernel and coconut shells turned out to be a prominent nuisance to the environment and their disposal was a major challenge especially in the south-east, south-west, south-south and parts of the middle belt regions of Nigeria. Recently, they are now being processed and bagged

for export outside the country. In view of this, their conversion to activated carbons for application in energy storage device, water purification and environmental remediation should be a welcome idea especially in this era of global energy crisis and quest for clean portable water in most rural areas of the developing countries. Activated carbon is a microcrystalline, non-graphitic form of carbon with much more disordered structure compared to that of graphite. X-ray analysis of the structure showed that the crystallites are only a few layers in thickness and are less than 10 nm in width [1]. The micro-porous structure; with a large internal surface area ranging from 250 - 2500 m^2/g, occupying the spaces between the crystallites of activated carbon allow it to preferentially adsorb organic materials and other nonpolar compounds from gas or liquid streams. These unique structural characteristics have been exploited by researchers around the globe for water purification [2, 3, 4, 5, 6] and energy storage potentials [7, 8, 9, 10, 11, 12].

The use of activated carbon to absorb microbes, organic matter and its likes has been established in many research efforts around the globe and its use could also prevent the problem of chlorine decay and formation of by-products; in the water distribution networks, claimed to be responsible for cardiovascular diseases, cancers, and birth defects [6, 13, 14, 15, 16]. The fear of these diseases coupled with the high cost of importing chlorine in developing countries calls for the use of activated carbon as a cheaper and eco-friendly point of use water filters. In recent times, the quest for production of efficient, low-cost, scalable, locally available and renewable carbon materials for absorbent and energy storage applications has shifted the attention of most researchers to the use of agricultural or organic waste materials for the production of activated carbon [17]. In view of this, our choice of coconut and palm kernel shells is tied to the inherent possession of high carbon content, high density and hardness which are ideal for the manufacture of hard granular activated carbon with very low ash and sulphuric contents useful for a wide range of applications not limited to the removal of contaminants and adsorption of small molecular weight species [18, 19, 20], but includes energy storage capabilities.

Nevertheless, research efforts on the use of activated carbons derived from coconut shell and pine cone and others like expanded graphite, carbon nanotubes, graphene, conducting polymer etc. for supercapacitor electrode have been reported [7, 8, 9, 10, 11, 12]. However, Several supercapacitor systems based on activated carbon, carbon nanotubes and graphene electrode have been developed to attain high performance energy storage devices namely; AC//$Ni(OH)_2$ [21], graphene//$Ni(OH)_2$ [22], carbon nanotubes//MnO_2 [23], AC//MoO_3 [24].

Though, these electrochemical supercapacitor systems exhibited high energy storage capabilities but these are still far from commercialization due to the poor capacitive performance of the positive electrode materials at high current loading and the corresponding carbon negative electrode materials in a low current utilization [22].

In this work, we have demonstrated that activated carbon could be produced via microwave-assisted activation at a much shorter time (ranging from 5-10 min) and reduced cost compared to the conventional activation method embraced by most researchers for the production of activated carbons. We have also employed techniques such as thermo-gravimetric analysis, Fourier Transform Infra-red spectroscopy, surface adsorption measurement, scanning electron microscopy, X-ray diffraction analysis, cyclic voltammetry and electrochemical impedance spectroscopy to study the physical properties (such as density, moisture content and ash content), thermal property, structure, surface functionalities, adsorption capability and electrochemical characteristics. The choice of the co-activators in this work was informed by the fact that they are more eco-friendly compared to the $ZnCl_2$, H_3PO_4 and many more that are frequently used. Finally, the choice of activation technique is also tied to the established fact that microwave technology leads to decreased reaction time and increased productivity yield of materials compared to the conventional heating system [25, 26, 27, 28, 29, 30].

Materials and Methods

The coconut shells were obtained from an open market in Sabon-Gari market, Zaria, Kaduna State, Nigeria where they were being dumped as a waste product while the palm kernel shells were obtained from a farm in Osolo area near Odo-Oba in Iwo LGA, Osun State, Nigeria. The coconut and palm kernel shells were washed with distilled water and dried for 24 hours in ambient air. These raw materials were subsequently crushed, pulverized and sieved through mesh of 125 μm to obtain a fine particle size powder and remove unwanted particles. Two samples of the mixture of coconut and palm kernel shells were prepared containing 5g each of palm kernel and coconut shells.

The chemical activation of the sample for water filter was achieved via a two-stage microwave heating involving partial thermal decomposition of the raw material in $0.1M$ solution containing varying concentration of sodium chloride and glycine (amino acetic acid) and subsequent activation of the derivative in $0.1M$ solution containing varying concentration of calcium chloride and ethylene glycol. The volumetric concentration of calcium chloride was 90, which

reflects that the initial volumetric concentration of sodium chloride was 10 and the sample was labeled (CS+PS). The complete activation process for the sample was achieved in 10 minutes with maximum microwave power of 2450 *W* at a frequency of 50 *Hz*.

Subsequently, the chemical activation of the sample for supercapacitor electrode was also achieved via a two-stage microwave heating involving partial thermal decomposition of the raw material in 0.1*M* solution containing varying concentration of potassium hydroxide and glycine (amino acetic acid) and subsequent incorporation of nanosized NiO filler and activation of the derivative in 3*M* KOH solution. The nano-sized nickel oxide was prepared from 1M solution containing $NiCl_2$ and Glycine in the presence of 3M KOH bath using microwave-assisted coprecipitation technique [28, 31, 32]. The precipitated gel was washed thoroughly with NH_4OH and subsequently heated for 2 minutes using microwave power (2450 *W*) to yield pure sample of nanosized NiO powder. In order to prepare the metal oxide filled activated carbon, the carbonized sample $(CS+PS)_F$ was mixed with nano-sized NiO powder in the ratio 9:1 by weight and subsequently impregnated with 3M KOH solution. The dissolved sample was carbonized for another 4 min using microwave power of 2450 *W* at a frequency of 50 *Hz*.

After carbonization, the activated carbon samples were washed thoroughly with mixture of distilled water and ammonia solution to eliminate the residual activating agent that must have penetrated into the pore spaces and occupied substantial volume of the activated carbon samples. This was done to create large numbers of pore spaces. Subsequently, the activated carbon samples were ground to fine particle sizes and re-heated for a minute to further activate the carbon samples. Finally, the metal oxide filled activated carbon sample $(CS+PS)_F$ and the activated carbon sample without filler (CS+PS) were ground again to fine particle sizes.

The bulk density and thermo-gravimetric analysis of the activated carbon samples were measured using Micromeritic AccuPyc II 1340 (version 1.03). The structures and functional groups of the produced activated carbons were elucidated using X-ray Diffractometer (PANALYTICAL XPERT PRO), which was equipped with Cu-K_α radiation (40 kV, 30 mA) with a 0.02º step size and 2.5 second step time over the range $10º < 2\theta < 70º$ and Fourier Transform Infrared Spectrophotometer (SHIMADZU FTIR-8400S). The morphology and elemental composition of the produced activated carbons were investigated using Scanning Electron microscope (FEI QUANTA 2020). The effectiveness of the activated carbon for removal of organic dye (methylene blue) from water contaminated with the organic dye was tested via adsorption studies using the Freundlich model. For the activated carbon sample with nano-filler, electrochemical measurements; such as Cyclic Voltammetry (CV), Galvanostatic Charge-Discharge (GCD) and electrochemical impedance spectroscopy (EIS) were carried out using a Bio-logic SP-300 Potentiostat. The three electrode method was employed; where the Activated Carbon (AC) sample with nano-filler serves as the working electrode, Glassy Carbon Plate (GCP) as the counter electrode and Ag/AgCl (3M KCl) serves as reference electrode in 6M KOH electrolyte. The AC electrode was prepared using Polyvinylidene Flouride (PVDF) as a binder and N-methylpyrolidine (NMP) solution as dispersant. The active material (AC) and

Polyvinylidene Flouride (PVDF) were mixed in ratio 9:1 by weight respectively, homogenized and dispersed in N-methylpyrolidine (NMP) solution. The paste was then uniformly attached on a nickel foam current collector and dried at 60^{o}C in an oven for 8 hours to ensure evaporation of the NMP and then allowed to cool down to room temperature. Cyclic voltammetry (CV) was performed by scanning the potential from - 0.3 to + 0.2 V and the rates were varied from 25 to 100 mVs^{-1}. The charge-discharge analysis was carried out at four different constant currents of 2.5, 5.0, 7.5 and 10.0 mA at potential range of 0 to 0.5 V. Finally, the Electrochemical Impedance Spectroscopic (EIS) study of the three electrode assembly was performed in 6M KOH aqueous solution applying a sinusoidal signal of 10 mV peak-to-peak amplitude at a frequency range of 100 mHz to 100 kHz. The impedance data were analyzed in terms of complex impedance using the imaginary and real part plots for the sample $(CS+PS)_F$.

Results and Discussions

The measured density of the activated carbon for supercapacitor electrode $(CS+PS)_F$ was obtained to be $(1.8862 \pm 0.0002) g\,cm^{-3}$ while that for water filter was obtained to be $(2.185 \pm 0.0025) g\,cm^{-3}$. The measured bulk density revealed that the activated carbon for water filter is denser than nano-sized nickel oxide filled activated carbon for supercapacitor electrode. This is attributed to the fact that there are more pores in the structure of the nano-sized nickel oxide filled activated carbon giving it better storage capability. The thermo gravimetric analysis (TGA) results also revealed that nano-sized nickel oxide filled activated carbon is more resistant to thermal shock at elevated temperature compared to activated carbon for water filter. The residual mass of nano-sized nickel oxide filled palm kernel shell after series of thermal cycles at $817.46^{o}C$ was *45.83%* which is higher than that for activated carbon for water filter as depicted in the TGA plots. It has been established that moisture and ash contents of activated carbon should be low if it must be used for adsorption and catalytic applications. Low content of ash and moisture in activated carbon is indicative of the quality and kind of activated carbon produced. The moisture content for the samples ranges from 6.50% to 7.21%. The moisture content is less than 10% for both nano-sized nickel oxide filled activated carbon sample and activated carbon sample for water filter which is in conformity with the results in the work [33] and also indicative of low moisture absorption by the samples. Similarly, the ash content in each case is less 5% about 4.22% for nano-sized nickel oxide filled activated carbon sample and about 3.66% for the activated carbon sample for water filter.

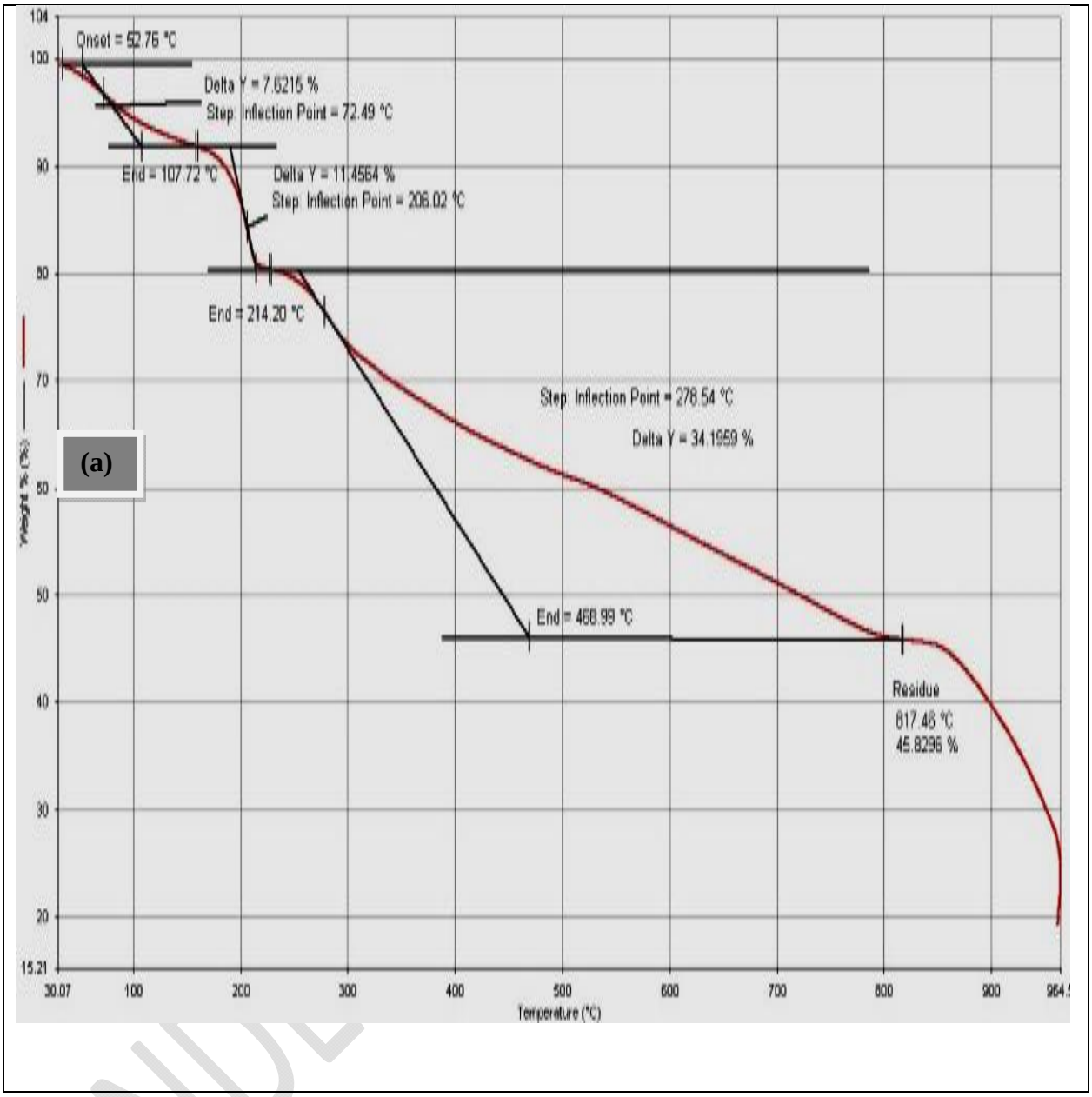
Onset = 52.76 °C
Delta Y = 7.6216 %
Step: Inflection Point = 72.49 °C
End = 107.72 °C
Delta Y = 11.4564 %
Step: Inflection Point = 206.02 °C
End = 214.20 °C
Step: Inflection Point = 278.54 °C
Delta Y = 34.1959 %
End = 468.99 °C
Residue
817.46 °C
45.8296 %
(a)
Weight (%)
Temperature (°C)
104
100
90
80
70
60
50
40
30
20
15.21
30.07
100
200
300
400
500
600
700
800
900

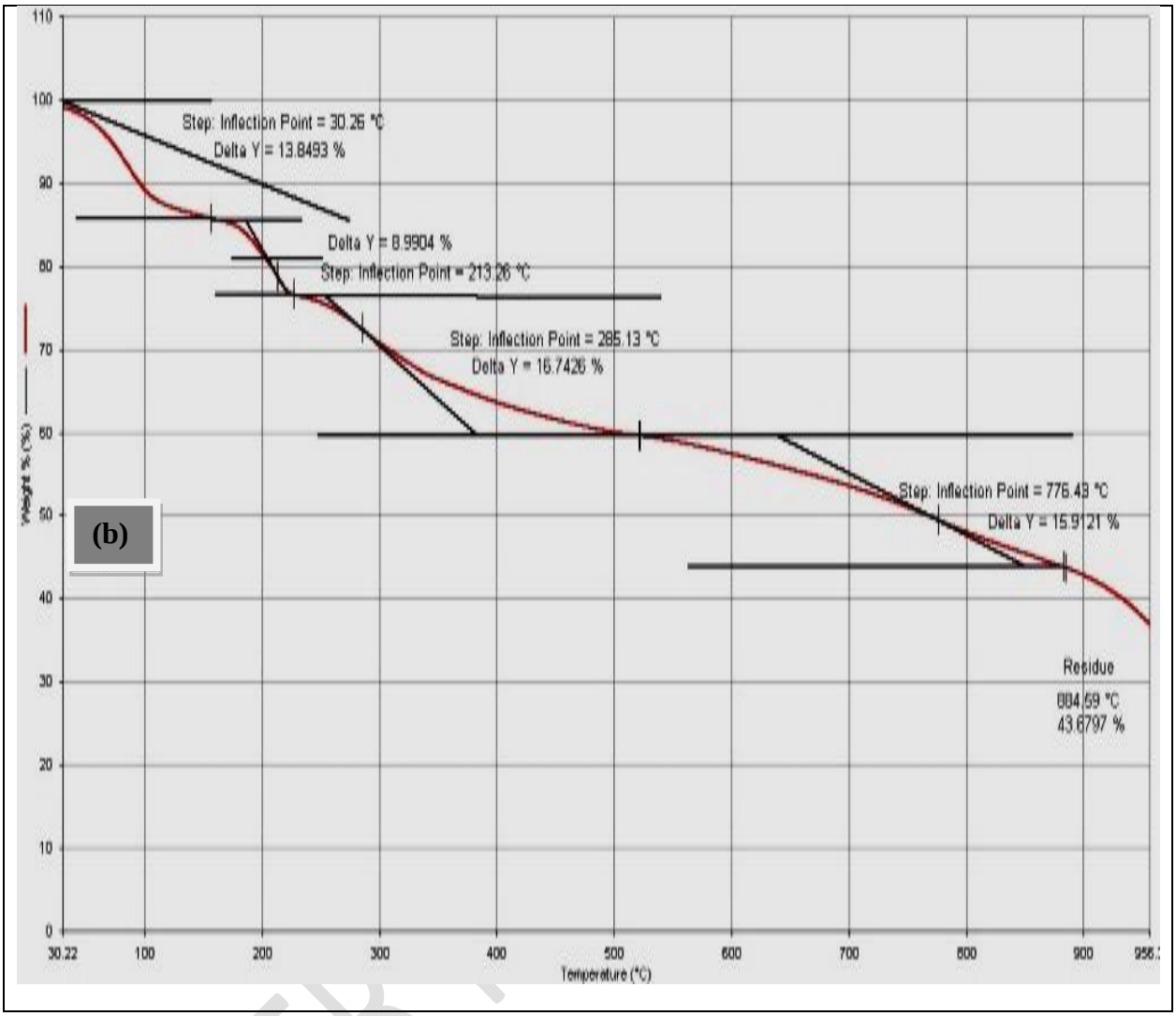

Fig.1. TGA Plots for (a) Nano-sized nickel oxide filled activated carbon $(CS+PS)_F$ and (b) Activated carbon for water filter (CS+PS).

The FTIR spectra for the raw powder sample (PCS+PPS) and the activated carbon mixture of coconut shell and palm kernel shell (CS+PS) and nano-sized nickel oxide filled activated carbon mixture of coconut shell and palm kernel shell $(CS+PS)_F$ samples are presented in Figure 2. Table 1 summarises the results obtained from FTIR spectroscopy for the raw powder sample (PCS+PPS), nano-sized nickel oxide filled activated carbon mixture of coconut shell and palm kernel shell $(CS+PS)_F$ and activated carbon mixture of coconut shell and palm kernel shell (CS+PS). The FTIR spectral were interpreted by assigning functional groups to their corresponding absorption bands and these are discernable by their corresponding peak values. The prominent functional groups in the samples are basically the hydroxyl groups, alcohols and

carbonyl groups comprising of OH stretching vibrations, CH_2 stretching and bending vibrations, CH_3 bending vibrations, C-OH stretching and bending vibrations, CH bending and C=O stretching vibration.

The FTIR spectra display broad bands at *3200 cm^{-1} - 3946.49 cm^{-1}*, which are believed to be associated with the stretching vibrations of hydrogen bonded surface water molecules and hydroxyl groups. In addition to the broad band representing the stretching vibrations of hydrogen bonded surface water molecules and hydroxyl groups occurring at 3418.94 cm^{-1}, there exists a band spanning the range 1622.19 cm^{-1} -1400.37 cm^{-1} associated with OH bending vibration implying the existence of lattice water. The band at *1612.54 cm^{-1} – 1710.92* cm^{-1} is associated with non-conjugated *C=O* stretching vibration implying the existence of carbonyl absorptions. The changes observed in the vibration frequency of *vC=O* in the activated carbon samples indicate that the incorporation of the co-activators and NiO has great influence on the vibration frequency of *vC=O*. In the case of nickel oxide filled activated carbon mixture of coconut shell and palm kernel shell, the disappearance of the functional group indicates that the addition of NiO has suppressing tendency on the vibration frequency of vC=O because of conjugation with organic groups (vCH_2). The band in the range *1383.01 cm^{-1}* associated with CH bending vibration implies the existence of secondary alcohols. In addition, the bands at *546.84 cm^{-1}-1039.74 cm^{-1}* are associated with *C-OH* bending and stretching vibrations of the secondary alcohols. The shift to higher frequencies may be attributed to additional bonding of these groups with metallic compounds. Finally, the functional group appearing at 447.5cm^{-1} represents Ni-O stretching vibration and that appearing in the range *425.32 cm^{-1}* represents *Ca-O* stretching vibration. Furthermore, the small absorptions observed for the organics indicates their presence in minute quantities on the surfaces of the metal oxide filled activated carbon.

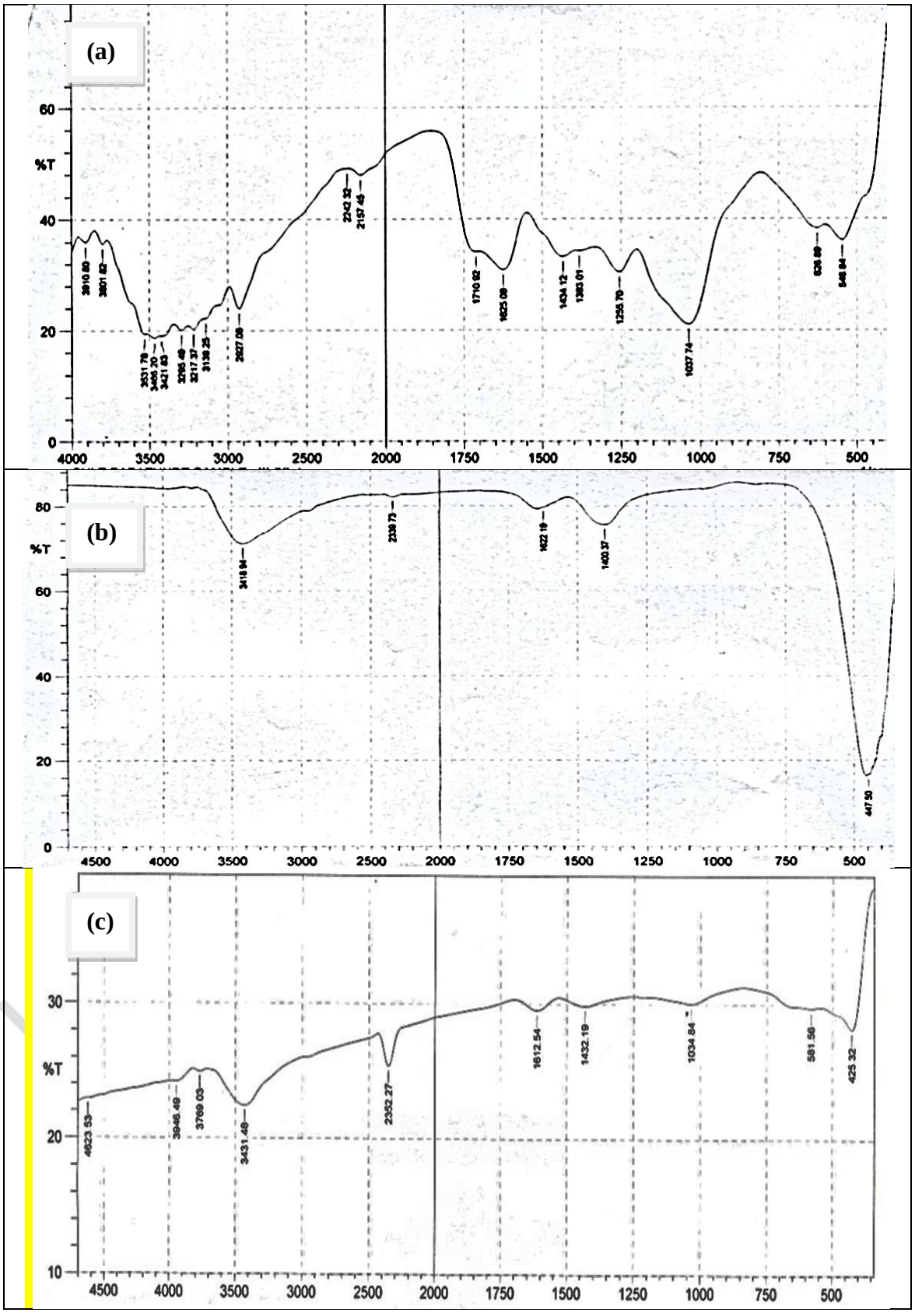
(a)
%T
60
40
20
0
4000
3500
3000
2500
2000
1750
1500
1250
1000
750
500
3910.80
3801.82
3531.78
3466.20
3421.83
3265.49
3217.37
3138.25
2927.08
2242.32
2157.45
1710.92
1625.08
1434.12
1383.01
1258.70
1037.74
638.89
546.84
(b)
%T
80
60
40
20
0
4500
4000
3500
3000
2500
2000
1750
1500
1250
1000
750
500
3418.94
2339.73
1622.19
1400.37
447.50
(c)
%T
30
20
10
4500
4000
3500
3000
2500
2000
1750
1500
1250
1000
750
500
4623.53
3946.49
3769.03
3431.46
2352.27
1612.54
1432.19
1034.84
581.56
425.32

Fig.2. FTIR Spectra of (a) Powdered mixture of coconut shell and palm kernel shell (PCS+PPS), (b) Nano-sized nickel oxide filled activated carbon mixture of coconut shell and palm kernel shell $(CS+PS)_F$ and (c) Activated carbon mixture of coconut shell and palm kernel shell (CS+PS)

Table 1. Band assignment of the peaks obtained from the FTIR spectra for the raw material samples and activated carbon samples.

Band Assignment	**Absorption Band (cm^{-1})**		
	Raw Sample	**Activated Samples**	
	PCS+PPS	**$(CS+PS)_F$**	**(CS+PS)**
Intermolecular Hydrogen Bonding (OH stretching vibration)	3200-3512.49	3418.94	3431.48-3946.49
Free NH stretching vibrations	3139.25	-	-
CH_2 (CH stretching vibration)	2927.08	-	-
Non-Conjugated (C≡N stretching vibration)	2242.32	2338.73	2352.20
Non-Conjugated (C=O stretching vibration)	1710.92	-	1612.54
OH (bending vibration)	1625.08	1622.19	-
CH_2 (CH bending vibration)	1434.12	1400.37	1432.19
CH_3 (CH bending vibration)	1383.01	-	-
C-OH stretching vibration	1039.74	-	1034.84
C-OH (OH bending vibration)	546.84	-	581.56
Ni-O (stretching vibration)	-	447.5	-
Ca-O (stretching vibration)	-	-	425.32

Figure 3(a & b) shows SEM micrographs of nickel oxide filled activated carbon mixture coconut shell and palm kernel shell $(CS+PS)_F$ and activated carbon mixture of coconut shell and palm kernel shell (CS+PS). The figure depicts high magnification images revealing highly porous structures needed for fast ion transport in high performance supercapacitors and water purification. The variation in contrast of the images revealed the $(CS+PS)_F$ samples to be a two-

phase system interspersed by nickel oxide. The dark phase associated with the host matrix (activated carbon) is overlaid by the light phase associated with the filler (nickel oxide). As for the (CS+PS), the host matrix which appear to be layered crystallites is overlaid by the light phase associated with the CaO (remnant of the activator). The resultant particle size analysis was obtained using imaging software (Image-J) and this revealed the average particle size for nickel oxide filled activated carbon mixture of coconut shell and palm kernel shell to be (108.24±44.33) nm and the crystallite size for the activated carbon mixture of coconut shell and palm kernel shell to be (72.78±0.76) μm.

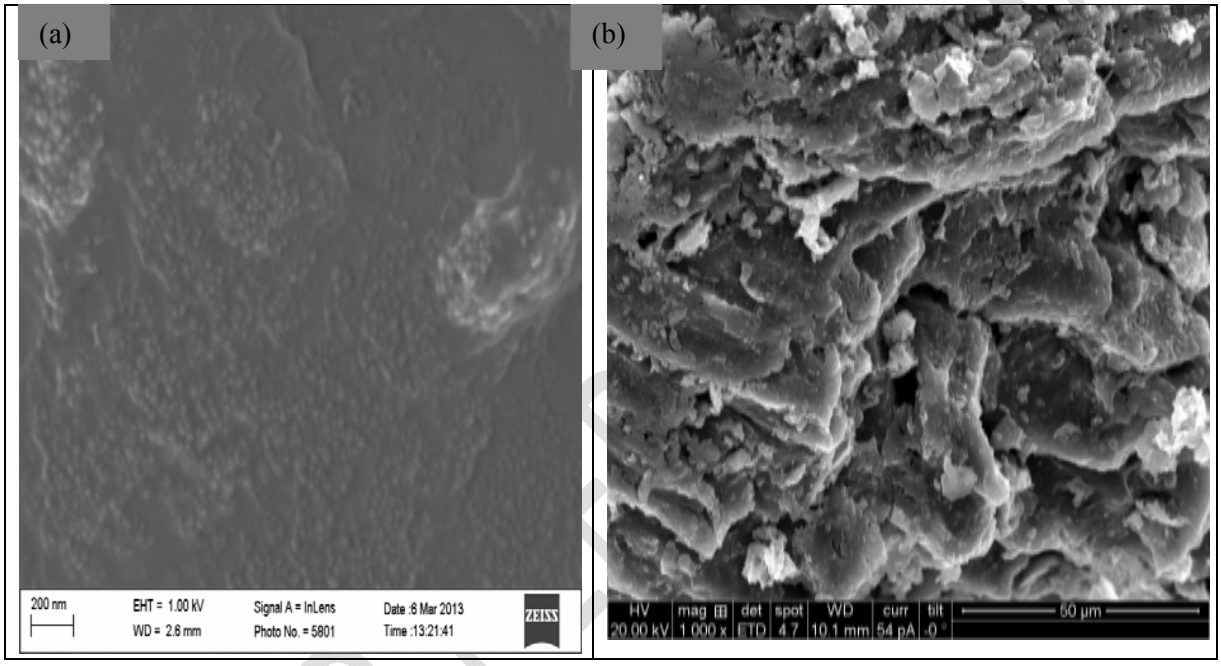

Fig.3. SEM Micrograph for (a) Nickel oxide filled activated mixture of coconut shell and palm kernel shell and (b) activated mixture of coconut shell and palm kernel shell without filler.

The XRD pattern (black) shown in Figure 4 for the activated carbon mixture of coconut shell and palm kernel shell is characterized by reduced number of peaks compared to the XRD pattern (red) for the nickel oxide filled activated carbon mixture of coconut shell and palm kernel shell. This could be attributed to the high content of amorphous activated carbon phase identified to be disordered synthetic graphite structure. Whereas the degree of crystallinity in the nickel oxide filled activated carbon mixture of coconut shell and palm kernel shell is high. This could be attributed to the presence of ordered graphite structure and nickel oxide and the XRD peaks are identified to graphite and nickel oxide peaks. In the XRD patterns depicted in Figure 4, the most prominent peak used to identify graphite structure occurs at $2\theta = 25^{o}$, but in the XRD pattern (black) for the (CS+PS), a broad peak at $2\theta = 23^{o}$ and 43^{o} revealed amorphous graphitic carbon phase. The crystalline peaks occurring at 26^{o}, 29^{o} and 32^{o} (PDF 1-0338) in the XRD pattern (black) for (CS+PS) represent synthetic $CaCl_2$. In the XRD pattern (red) for the

$(CS+PS)_F$, the peak positions described by 2θ= 28°, 32°, 45°, 55° and 76° (JCPDS: 00-008-0415) are associated with ordered graphitic carbon phase. While the most prominent crystalline phases associated with nickel oxide occur at the following 2θ = 36°, 44°, 63°, 79° (JCPDS: 22-1189) and nickel hydroxide at the following 2θ = 10°, 23°, 34°, 59°, (JCPDS: 38-0715).

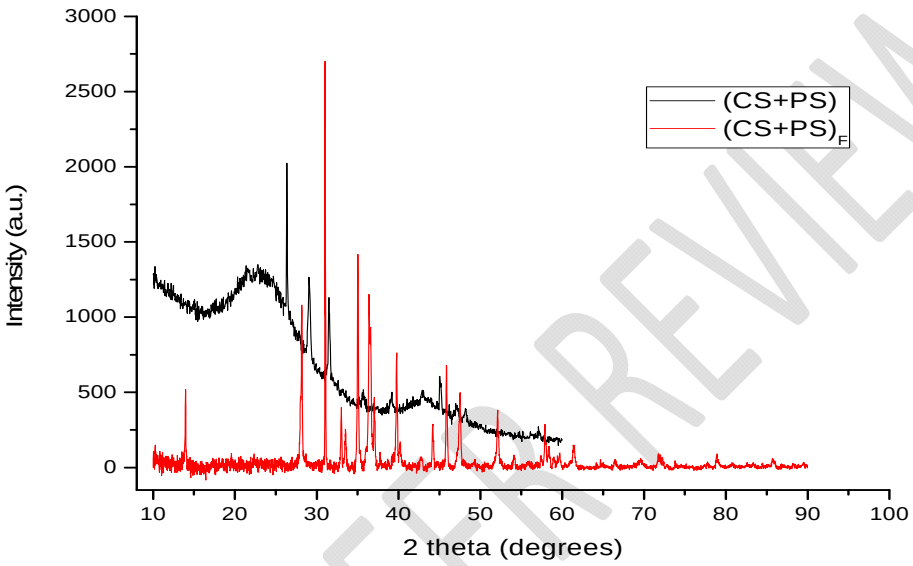

Fig.4. XRD pattern for (a) activated mixture of coconut shell and palm kernel shell without filler (black line) and (b) Nickel oxide filled activated mixture of coconut shell and palm kernel shell (red line).

Figure 5 depicts the adsorption capacities of the activated mixture of coconut shell and palm kernel shell (CS+PS) and the absorbed amount of Methylene blue (MB) by the sample. The equilibrium adsorption data were interpreted using Freundlich models. The applicability of this model was established from the obtained value of the correlation coefficient, R^2=0.90. The obtained value of the correlation coefficient is in good agreement with the model because the isotherm for activated mixture of coconut shell and palm kernel shell (CS+PS) bear a resemblance to that of Freundlich isotherm. Thus, this shows that the activated mixture of coconut shell and palm kernel shell (CS+PS) exhibited distinctive multilayer adsorption capability as against monolayer coverage. The obtained results reflect that the activated mixture of coconut shell and palm kernel shell (CS+PS) favourably adsorbed MB dyes. The overall assessment of the activated mixture of coconut shell and palm kernel shell (CS+PS) reveals Freundlich model to be more suitable for the interpretation of the experimental adsorption data as the correlation coefficient value for the activated mixture of coconut shell and palm kernel shell

(CS+PS) was not more than 0.90. The overall absorption capacity was found to be 290mg.g-^{1}. These values are in good agreement with literature [34]. As such, the activated mixture of coconut shell and palm kernel shell (CS+PS) exhibited a very good adsorption capacity for MB and is paraded with better micro porous structure suitable for filtration.

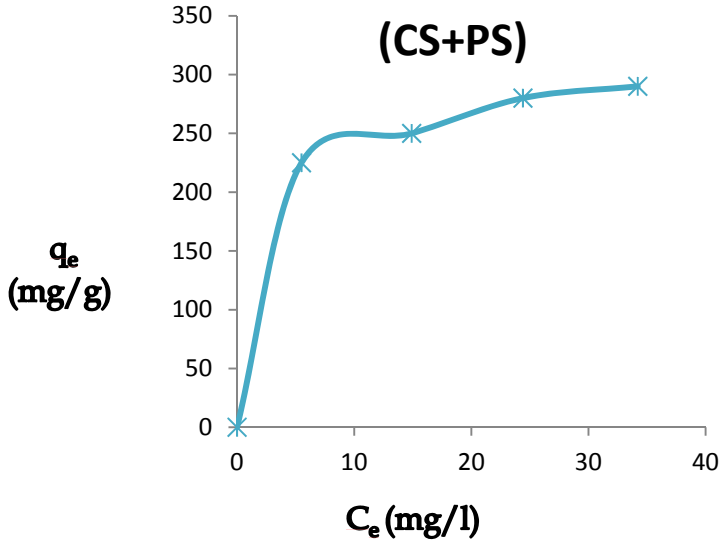

Fig.5. Adsorption capacity of (CS+PS) activated carbon for methylene blue.

Nyquist plot for the supercapacitor cell assembly based on nickel oxide filled activated carbon mixture of coconut shell and palm kernel shell $(CS+PS)_F$ in 6M KOH aqueous solution is presented in Figure 6 with an inset showing the expanded high frequency region of the same plot. It can be seen from Figure 6 and the inset, that the cell shows a pronounced semicircle at high frequency implying the charge transfer controlled regime and a straight line at low frequency indicating the capacitive regime. The impedance plot obtained for the supercapacitor cell assembly is in line with that of transmission line model (TLM) for the porous electrodes described in the literature [35].

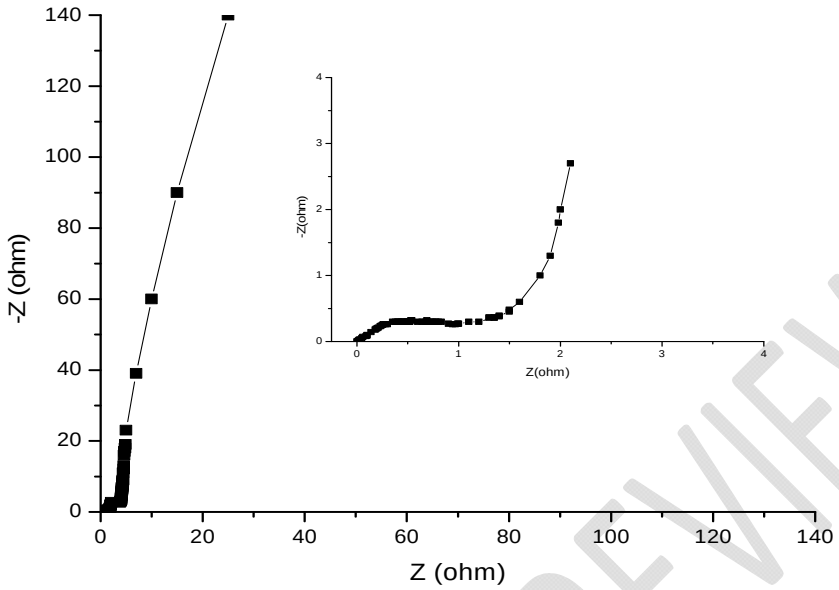

Fig.6. Electrochemical Impedance Spectroscopy for nickel oxide filled activated mixture of coconut shell and palm kernel shell

Figure 7 shows the cyclic voltammogram of the supercapacitor cell assembly based on nickel oxide filled activated carbon mixture of coconut shell and palm kernel shell $(CS+PS)_F$ in 6M KOH aqueous solution as the electrolyte. The figure depicts a rectangular shaped voltammogram with a large current separation and symmetric in both cathodic and anodic directions obtained for the cell assembly. The potential scan was varied from 25 to100 mV/s. A clear capacitive behaviour can be seen from the voltammograms; an established fact arising from the large current separation between the forward and reverse scans with no visible redox peak formation. It can also be seen that the voltammograms are symmetrical about the current zero axis. The fact that all the CVs show rectangular features at the selected scan rates with high current values indicates a good electrochemical activity and high power density.

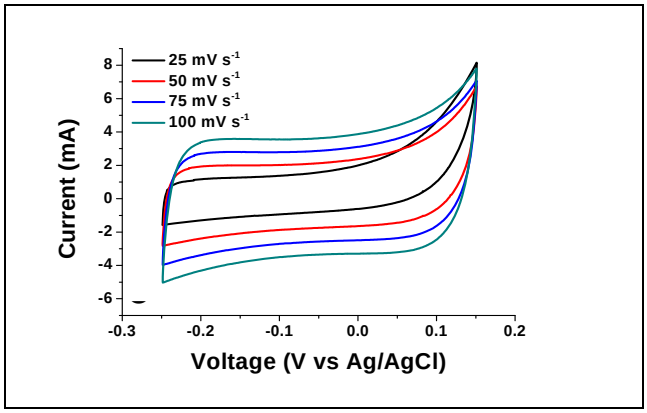

Fig.7. Cyclic voltammetry curves for nickel oxide filled activated carbon mixture of Coconut shell and Palm kernel shell $(CS + PS)_F$ at different scan rates

The galvanostatic charge-discharge analysis of the supercapacitor cell assembly was performed at four different current densities namely 2.5 mA to 10 mA and from this analysis, the charge storage capacity and durability of the cycle lifetime were obtained. Figure 8 shows the typical charge-discharge profiles of the supercapacitor cell assembly based on nickel oxide filled activated carbon mixture of coconut shell and palm kernel shell in 6M KOH aqueous solution. We have used voltage range of 0 to 0.5 V in order to evaluate the performance of the supercapacitors at different voltages. It can be seen that the charge – discharge profiles deviate from the typical linear variation of voltage with time normally exhibited by a purely electrochemical double layer capacitor (EDLC) for lower current values of 2.5 mA and 5.0 mA, which conforms to the proposed model described in the literature [35]. While the linear behaviour emanating at higher current values of 7.5 mA and 10 mA, is an indication of the formation of a good electrode/electrolyte interface with a well-defined conductivity.

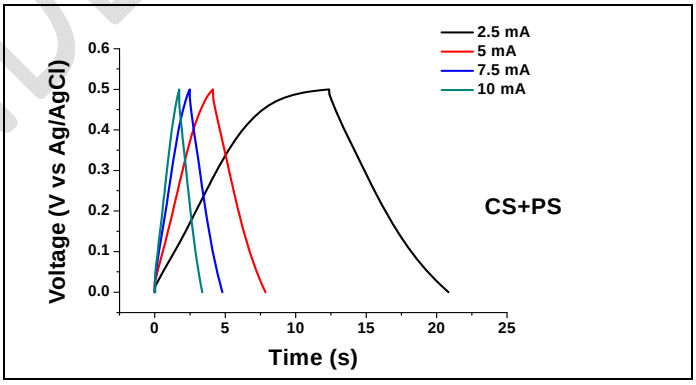

Fig.8. Galvanostatic charge-discharge curves for nickel oxide filled activated mixture of coconut shell and palm kernel shell $(CS + PS)_F$.

Figure 9 depicts the specific capacitance for the nickel oxide filled activated mixture of coconut shell and palm kernel shell supercapacitor assembly. A specific capacitance of 41 F/cm^2 was obtained at a constant current density of 2.5 mA/cm^2 for the supercapacitor cell assembly. In fact, the specific capacitance decreases to a large extent with the number of cycles for higher current densities to 40 F/cm^2 at 5mA/cm^2 and 7.5 mA/cm^2 and 32 F/cm^2 at 10mA/cm^2 for supercapacitor assembly. Thus, the supercapacitor cell assembly based on NOFAC palm kernel shell shows better electrochemical properties.

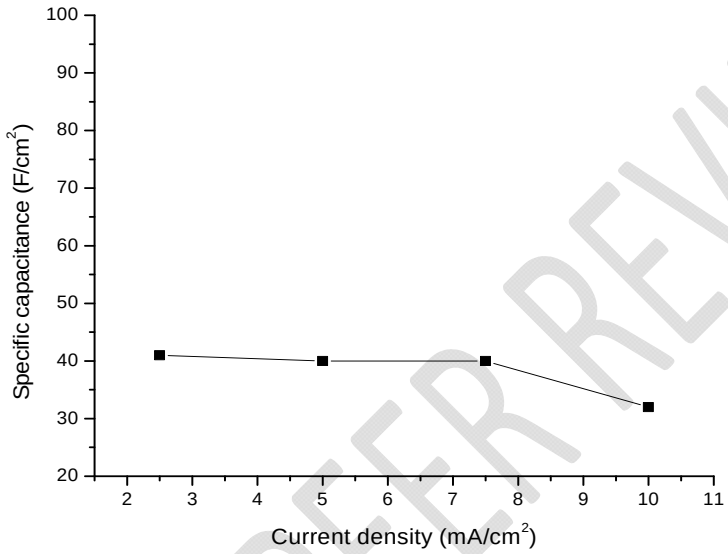

Fig.9. Specific capacitance for nickel oxide filled mixture of Coconut shell and Palm kernel shell $(CS + PS)_F$.

4.0 Conclusions

The microwave-assisted activation technique has been successfully adopted for the production of nickel oxide filled activated carbon mixture of coconut shell and palm kernel shell $(CS+PS)_F$ and activated carbon mixture of coconut shell and palm kernel shell (CS+PS) for supercapacitor electrode and water purification. The FTIR spectroscopy results for $(CS+PS)_F$ confirmed the existence of strong interfacial interaction between NiO and the host matrices showing creation and annihilation of absorption bands in the IR spectra. This interaction revealed the existence of NiO oxide as an inclusion in the $(CS+PS)_F$ with significant absorptions observed below 500cm^{-1}. In addition to the functional groups associated with organics for (CS+PS), the significant absorptions observed below 500cm^{-1} revealed the existence of CaO as remnant in the (CS+PS). The high magnification SEM images revealed highly porous structures required for fast ion transport in high performance supercapacitors and water purification. The XRD analysis

confirmed the activated carbon mixture to be polymorphic systems with all the XRD peaks identified to be graphite, nickel oxide, nickel hydroxide and calcium chloride structures. The adsorption studies on (CS+PS) revealed that Freundlich model is most suitable for the interpretation of the adsorption data. As such, the activated mixture of coconut shell and palm kernel shell (CS+PS) exhibited a very good adsorption capacity for MB and is paraded with better micro porous structure suitable for filtration. The cell assembly tested in this study attained very good electrochemical performance based on common techniques for testing electrodes such as cyclic voltammetry (CV), Galvanostatic charge/discharge (GCD), and electrochemical impedance spectroscopy (EIS). A rectangular shaped voltammogram with a large current separation and symmetric in both cathodic and anodic directions for the cell assembly indicate a clear capacitive behaviour, a 1od electrochemical activity and high power density. The specific capacitance values of 44 F/cm^2, 40 F/cm^2, 40 F/cm^2 and 32 F/cm^2 were obtained at 2.5mA/cm^2, 5mA/cm^2, 7.5mA/cm^2 and 10mA/cm^2 respectively for the supercapacitor assembly based on nickel oxide filled activated coconut shell and palm kernel shell $(CS+PS)_F$. In this study, $(CS+PS)_F$ is paraded with better current response, higher value of specific capacitance and better electrochemical behaviour can be used for production of supercapacitor electrodes.

References

1. Smisek M, Cerney S. Active Carbon Manufacture, Properties and Applications. Elsevier Pub., Comp., New York, 1970; 5: 562-563.

2. Ofomaja AE, Naidoo EB. Bisorption of Copper from Aqeous solution by Chemically Activated Pine Cone: A Kinetic Study. Chem. Eng. J. 2011; 175: 260-270.

3. Momcilovic M, Purenovic M, Bojic A, Zarabica A, Randelovic M. Removal of Lead (II) ions from Aqueous Solutions by Adsorption onto Pine Cone Activated Carbon. Desalination. 2011; 276: 53-59.

4. Ge X, Tian F, Wu Z, Yan Y, Cravotto G, Wu Z. Adsorption of naphthalene from aqeous solution on coal-based active modified by microwave induction: Microwave power effect. Chem. Eng. Process. Process Intensif, 2015; 91:67-77.

5. Nunell GV, Ferdinandez ME, Borelli PR, Cukierman AL. Nitrate Uptake improvement by Modified Activated Carbons Developed from Two Species of Pine Cone. J. Colloid Interface Sci., 2015; 440: 102-108.

6. Ahmed TO, Galadima IA, Egila FE, Aliyu S. Activated carbon from mixture of coconut and palm kernel shells via microwave-assisted activation for water purification. Proceedings of the 15th Annual Conference of Materials science & technology Society of Nigeria (MSN), A. Giwa (ed.), 2016; 367-373.

7. Taberna PL, Simon P, Fauvarque J-FF. Electrochemical Characteristics and Impedance Spectroscopy Studies of Carbon-Carbon Supercapacitors. J. Electrochem. Soc., 2003; 150: A292-A300.

8. Roberts ME, Wheeler DR, McKenzie BB, Bunker BC. High Specific Capacitance Conducting Polymer Supercapacitor Electrodes based on Poly [tris(thiophenylphenylamine)]. J. Mater. Chem., 2009; 19: 6977-6979.

9. Demarconnay L, Raymundo-Pinero E, Begiun F. Adjustment of Electrodes Potential Window in an Asymmetric Carbon/MnO_2 Supercapacitor. J. Power Sources. 2011; 196: 580-586.

10. Zhang W, Ma C, Fang J, Cheng J, Zhang X, Dong S. Asymmetric Electrochemical Capacitors with High Energy and Power Density based on Graphene/CoAl-LDH and Activated Carbon Electrodes. RSC. Adv., 2013; 3: 2483-2490.

11. Bello A, Barzegar F, Momodu D, Taghizadeh F, Fabiane M, Dangbegnon J. Morphological Characterization and Impedance Spectroscopy Study of Porous 3D Carbons based on Graphene foam-PVA/Phenol-formadehyde Resin Composite as an Electrode Material for Supercapacitors. RSC. Adv., 2014; 4: 39066-39072.

12. Ahmed TO, Ogunleye OO, Galadima IA, Sulle BA, Bello A. Electrochemical and structural characterization of nickel oxide filled activated carbon (NOFAC) for Supercapacitor Electrode Application. Nigerian Journal of Materials Science and Engineering (NJMSE). 2016.

13. Arbuckle T, Hrudey SE, Krasner SW, Nuckols JR, Richardson SD, Singer P, Mendola P, Dodds L, Weisel , Ashley, DL, Froese KL, Pegram RA, Schultz IR, Reif J, Bachand AM, Benoit FM, Lynberg MI, Poole C, Waller K. Assessing exposure in epidemiologic studies to disinfection by- products in drinking water: Report from an international workshop. Environ Health Perspect. 2002; 110(Suppl 1): 53– 60.

14. Bove F, Shim Y, Zeitz P. Drinking water contaminants and adverse pregnancy outcomes: a review. Environ Health Perspect. 2002; 110(Suppl 1): 61–74.

15. Woo YT, Lai D, McLain JL, Manibusan MK, Dellarco V. Use of mechanism-based structure–activity relationships analysis in carcinogenic potential ranking for drinking water disinfection by- products. Environ Health Perspect. 2002; 110(Suppl 1): 75–87.

16. Devarakonda V, Moussa NA, VanBlaricum V, Ginsberge M, Hock V. Kinetics of Free Chlorine decay in Water Distribution Networks; Proc. The World Environmental and Water Resources Congress, ASCE. 2010.

17. Park S, Liang C, Sheng D, Dudney N, DePaoli D. Mesoporous Carbon Materials as Electrode for Electrochemical Double Layer Capacitor. MRS Proc. 2006; 973: 903-916.

18. Hu Z, Srinivasan MP. Preparation of high-surface-area activated carbons from coconut shell, Micropor. Mesopor. Mater. 1999; 27: 11-18.

19. Ioannidou O, Zabaniotou A. Agricultural residues as precursors for activated carbon production--A review, Renew. Sustain. Ener. Revi. 2007; 11: 1966-2005.

20. Foo KY, Hameed BH. Microwave-assisted preparation of oil palm fiber activated carbon for methylene blue adsorption. Chem. Eng. J., 2011; 166(2): 792-795.

21. Wu MS, Hsieh HH. Nickel Oxide/Hydroxide Nanoplate synthesized by chemical precipitation for Electrochemical Capacitors. Electrochim. Acta., 2008; 53: 3427-3435.

22. Wang H, Casalongue HS, Liang Y, Dai H. Ni(OH)2 Nanoplates Grown on Graphene as Advanced Electrochemical Pseudocapacitor Materials. J. Am Chem. Soc. 2010; 132: 7472.

23. Aravanda LS, Bhat U, Ramachandra B. Binder free MoO3/Multi-walled Carbon Nanotube Thin film Electrode for High Energy Density Supercapacitor. Electrochim. Acta. 2013; 112: 663-669.

24. Tang W, Liu L, Tian S, Li L, Yue Y, Wu Y, Zhu K. Aqeuos Supercapacitor of High Energy Density based on MoO_3 Nanoplates as anode Material. Chem. Commun. 2011; 47: 10058-10060.

25. Menéndez JA, Menendez EM, Iglesias MJ, Garcia A, Pis JJ. Modification of the surface chemistry of active carbons by means of microwave-induced treatments. Carbon. 1999; 37(7): 1115-1121.

26. Nabais JM, Carrott PJM, Menendez JA. Preparation and modification of activated carbon fibers by microwave heating", Carbon. 2004; 42: 1315-1320.

27. Liu X, Yu G. Combined effect of microwave and activated carbon on the remediation of polychlorinated biphenyl contaminated soil. J. Hazard. Mater., 2006; 147: 746-751.

28. Kappe CO. Microwave Dielectric Heating in Synthetic Organic Chemistry. Chem. Soc. Rev., 2008; 37: 1127-1139.

29. Liu QS, Tong Z, Nan L, Peng W, Gulizhaer A. Modification of bamboo-based activated carbon using microwave radiation and its effects on the adsorption of methylene blue. Appl. Surface. Sci., 2010; 256(10): 3309-3315.

30. Liqiang Z, Mi M, Bing L, Yong D. Modification of activated carbon by means of microwave heating and its effects on the pore texture and surface chemistry, Journal of Applied Sciences, Engineering and Technology. 2013; 5(5): 1836-1840.

31. Baghbanzadeh M, Carbone L, Cozzoli PD, Kappe CO. Microwave-Assisted Synthesis of Colloidal Inorganic Nanocrystals. Angew, Chemie Int. Ed., 2011; 50: 1127-1139.

32. Mohammadyani D, Hosseini SA, Sadrnezhaad SK. Characterization of Nickel Oxide Nanoparticles Synthesisized via Rapid Microwave-Assisted Route. International Journal of Modern Physics: Conference Series. 2012; 5: 270-276.

33. Tiemey MJ, Prasertmanukitch S, Heslop S. Removal of Toluene with Dispersed-activated Carbon, J. Environ. Eng., 2006; 132, 350-357.

34. Bouchelta C, Medjram MS, Bertrand O, Bellat JP. Preparation and characterization of activated carbon from date stones by physical activation with steam. Journal of Analysis Applied Pyrolysis. 2008; 82: 70–77.

35. Conway CE. Electrochemical Supercapacitors: Scientific, Fundamental and Technologcial Applications. Kluwer Academic/Plenum, New York. 1999.